IWO # M9SF 99-0280

NUCLEAR ENERGY RESEARCH INITIATIVE (NERI) PROGRAM
~~DE-FG03-99SF0280~~, PNNL Project 32319
TECHNICAL PROGRESS REPORT
August – October 1999

Title: Novel Concepts for Damage-Resistant Alloys in Next Generation Nuclear Power Systems

Lead Investigating Organization: Pacific Northwest National Laboratory (PNNL), PO Box 999, Richland, WA 99352

PNNL Project Manager : S. M. Bruemmer

Collaborating Organizations: General Electric Corporate R&D, University of Michigan

Narrative:

Research Objective and Approach

The objective of the proposed research is to develop the scientific basis for a new class of radiation-resistant materials. Two approaches will be evaluated to develop damage resistant materials far superior to current stainless steels: (1) lattice perturbation to catalyze defect recombination within the early stages of cascade formation and defect migration and (2) controlled manipulation of the aggregate defect ensemble through the deliberate introduction of dynamic metastable microstructures. The intrinsic ability of the host matrix to resist displacement damage survival will be optimized in first concept. This approach (Task 1) explores baseline atomic displacement and recovery processes as affected by major and minor alloy constituents selected for the dual purpose of environmental cracking resistance as well as interactions with point defects. Inert oversized solutes known to improve corrosion behavior will be used to create vacancy/interstitial traps and promote defect recombination. Dynamic metastable microstructures tailored to resist damage accumulation will be investigated and optimized in the second concept (Task 2). Unique intermetallic second phases with inherent instabilities under irradiation will be used to create a dynamic microstructure resistant to radiation hardening, swelling and embrittlement. A key aspect of designing this dynamic microstructure will be to ensure the complex, radiation-induced changes do not promote environmental cracking.

The underlying radiation materials science for these two approaches is being explored using charged particle irradiations. Radiation damage resistance will be established by isolating the effect of each approach on defect microstructures, grain boundary microchemistries and matrix hardening. The dose dependence of these radiation-induced material changes will be used to identify promising alloys and initial microstructures that effectively delay or eliminate detrimental microstructural and microchemical evolution. Environmental cracking response is being established on non-irradiated alloys with thermomechanical treatments to simulate radiation microstructures and by tests on

DISCLAIMER

This report was prepared as an account of work sponsored by an agency of the United States Government. Neither the United States Government nor any agency thereof, nor any of their employees, make any warranty, express or implied, or assumes any legal liability or responsibility for the accuracy, completeness, or usefulness of any information, apparatus, product, or process disclosed, or represents that its use would not infringe privately owned rights. Reference herein to any specific commercial product, process, or service by trade name, trademark, manufacturer, or otherwise does not necessarily constitute or imply its endorsement, recommendation, or favoring by the United States Government or any agency thereof. The views and opinions of authors expressed herein do not necessarily state or reflect those of the United States Government or any agency thereof.

DISCLAIMER

Portions of this document may be illegible in electronic image products. Images are produced from the best available original document.

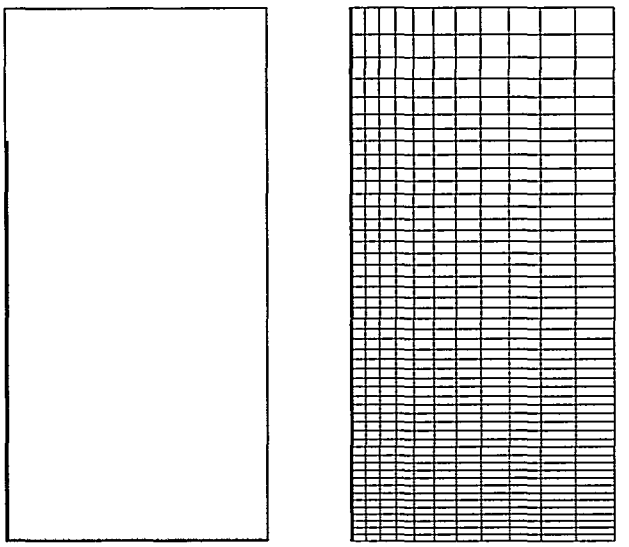

Figure 1: Initial configuration for a fractured material degradation with the 686 Finite Element mesh.

The Small-Crack Congestion Phenomenon

These developments provide a useful tool to investigate the effect of a crack network on the chemical degradation of cement-based materials. The case of a 2D-degradation of a rectangular cement paste of width 2 cm and length 4 cm is shown in Figures 1 to 3. A straight crack of half width 0.02 cm and length 3 cm is situated on the left side of the material. Figure 1 shows the initial conditions and the finite element mesh used in the analysis. The material is initially undegraded, and the degradation process starts from the bottom of the material where the aggressive boundary condition is prescribed. Figures 2 and 3 represent the solid calcium concentration in the material at times 5 and 15, and 30 and 50 years. The simulation results show the development of the degradation process and the propagation of the portlandite dissolution front as time flows. Figure 2 indicates that the portlandite dissolution front approximatively reaches the top of the crack after 15 years of leaching. The calcium solid concentration pattern at this time shows that the fracture (of high diffusivity compared to the solid matrix) is a preferential way of calcium evacuation from the material. However, and in contrast to the common assumption, the results also show that the preferential calcium evacuation path does not enhance the overall kinetics of material degradation. This new finding can be explained as follows:

The weak effect of the crack on the material deterioration can be attributed to the calcium congestion in the fracture due to the important quantity of calcium arriving from the material in the crack. Even if the diffusion process in the fracture was faster than the one in the material, the crack width would limit the number of calcium-ions that can be evacuated from the material through the crack to the outside. As a consequence, the calcium concentration in the fracture slowly decreases

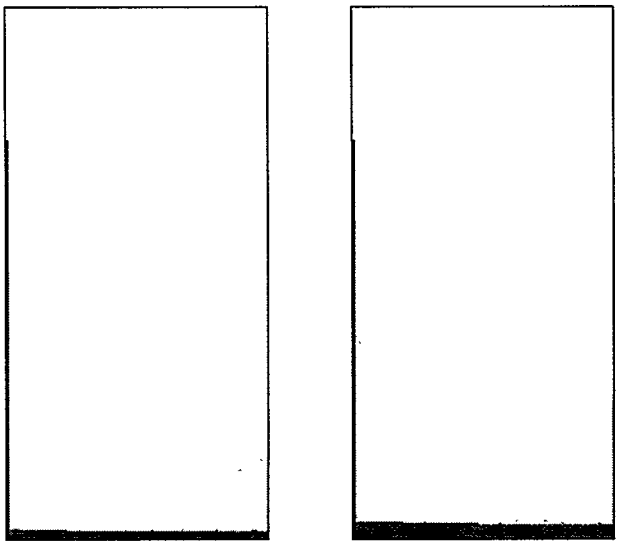

Figure 2: Solid calcium concentration at 5 and 15 years.

irrespective of the relative high diffusivity of the solution in the crack. To quantify this "crack congestion" effect, a dimensional analysis of a simplified model based on the dissolution of one mineral was performed (see [7]). This dimensional analysis reveals that the diffusion length in the fracture is of the form (for large values of time):

$$y_d(t) = C_1 \sqrt{\frac{bD_f}{\phi}} \left(\frac{t}{D_m}\right)^{1/4} \tag{1}$$

where b is the half fracture opening (crack width), D_f is the solute diffusion coefficient in the fracture, D_m is the effective diffusion coefficient in the matrix, ϕ is the material porosity and t is the time. The depth $\bar{y}_d$ defines the length in the fracture channel where the solute concentration has decreased from its initial value. Equation (1) indicates that a smaller fracture width $2b$, or a decrease of the diffusion coefficient D_f reduces the diffusion depth y_d. This is readily understood from physical evidence. In turn, a decrease of the porosity, ϕ, or a decrease of the material effective diffusion coefficient D_m leads to a larger diffusion depth y_d due to a smaller solute flux from the matrix into the fracture. However, in this case a smaller degradation depth in the perpendicular direction of the crack is found. Finally, in contrast to uncracked material, in which the dissolution front propagates as a function of the! squ are root of time (see the degraded depth at the border of the material at left in figure 4), the diffusion depth y_d in the fracture direction develops with the quadratic root of time. Hence, for large values of time, the material deterioration process due to a preferential calcium evacuation by diffusion in a thin crack can be neglected in comparison to the leaching process in the uncracked bulk material.

In summary, the diffusion through small cracks does not significantly affect the degradation process in the material even for large values of time. Our next focus will be

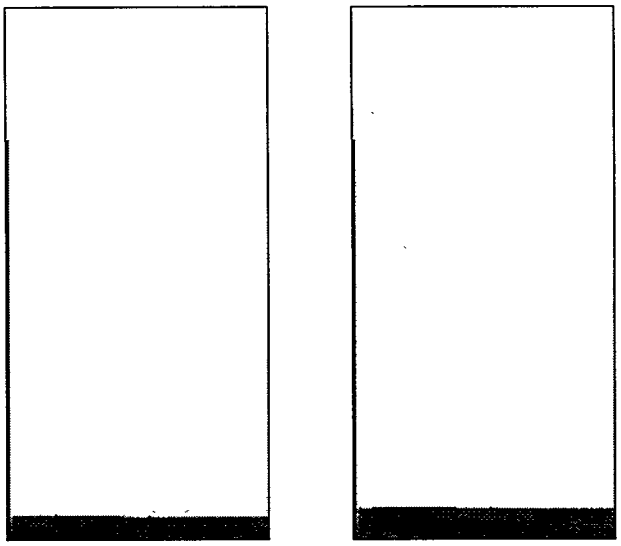

Figure 3: Solid calcium concentration at 30 and 50 years.

large cracks, in which a solute convection may provide a second transport mode for the evacuation of the solute concentration from the fracture. In this case, the "congestion phenomenon" observed and analyzed for small fractures may no more hold.

Task 3.1: Material testing

The objective of Task 3.1 is to determine the strength of leached cementious materials under triaxial stress states. This requires (a) an accelerated test method able to reproduce in vitro the intrinsic material response that characterizes the long-term behavior of cementitious materials; and (b) a homogeneous decalcification state to assess the "real" material response in the mechanical tests.

Design

Calcium leaching is a coupled diffusion - dissolution process that involves sharp dissolution fronts that propagate through the structure. Small sample sizes and high calcium efflux are necessary for a rapid leaching process. In the present study, the test program was carried out on pure cement pastes, the basic constituent of concrete, allowing for small and relatively homogeneous material samples. In addition, the calcium efflux can be artificially amplified by increasing the chemical equilibrium concentration, i.e. the calcium solubility, at the dissolution front. Leading to a higher calcium concentration gradient in the pore solution, and thus to higher efflux, this objective can be achieved by replacing the deionized water by an ammonium nitrate solution (See also last technical progress report). This type of leaching, which is equivalent to calcium leaching by pure water [2], leads to considerable acceleration of the front propagation velocity associated with the calcium dissolution process. As

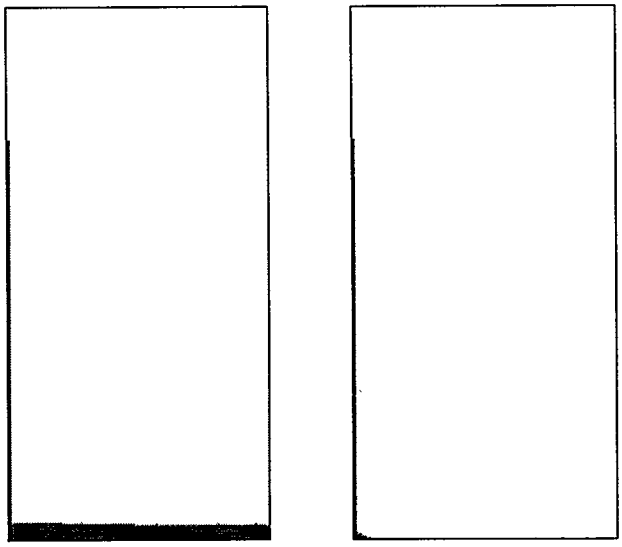

Figure 4: Solid calcium concentration at times 15 years with diffusion in the material along x-direction (left) and without (right).

a quasi-self similar diffusion-dissolution problem, the overall acceleration rate can be obtained from the ratio of the similarity parameter of front propagation:

$$a = \left(\frac{\xi_{d1}}{\xi_{d0}}\right)^2 \tag{2}$$

where $\xi_{d0} = x_d/\sqrt{t_0}$ and $\xi_{d1} = x_d/\sqrt{t_1}$ are close to a multiplied constant the self-similar parameters that define the position x_d of the dissolution front in the normal and accelerated leaching setting, respectively (see, e.g., [7]).

Calcium Leaching

The chosen Type I Portland cement paste samples with a water–cement ratio of $w/c = 0.5$ are cylinders of diameter 11.5 mm and length 60 mm. After 24 hours, the specimens were demoulded and cured in a saturated lime solution for 27 days at 20°C. One half of the samples were immersed in the 6M ammonium nitrate solution for accelerated leaching; the other half were stored for control purposes in limewater. To obtain good mixing of the ammonium nitrate solution and most homogeneous leaching conditions possible, the ammonium nitrate bath tanks were mounted on a slowly rotating table (see figure 5). In that way, the bath was constantly agitated and the sample surfaces were in free contact with the aggressive solution. Each tank of 15×15 cm quadratic shape was filled with 2.2 kg of aggressive solution and contained 26 specimens. In addition, carbonation by CO_2 was prevented by replacing the air in the tanks by pure nitrogen gas. In parallel, the pH of the solution was monitored. A necessary renewal of the solution due to a lack of Ammonium (NH_4^+) which slows down the leaching would have been indicated by a pH greater than 9.25. At the chosen combination of ammonium nitrate concentration, bath volume and number of

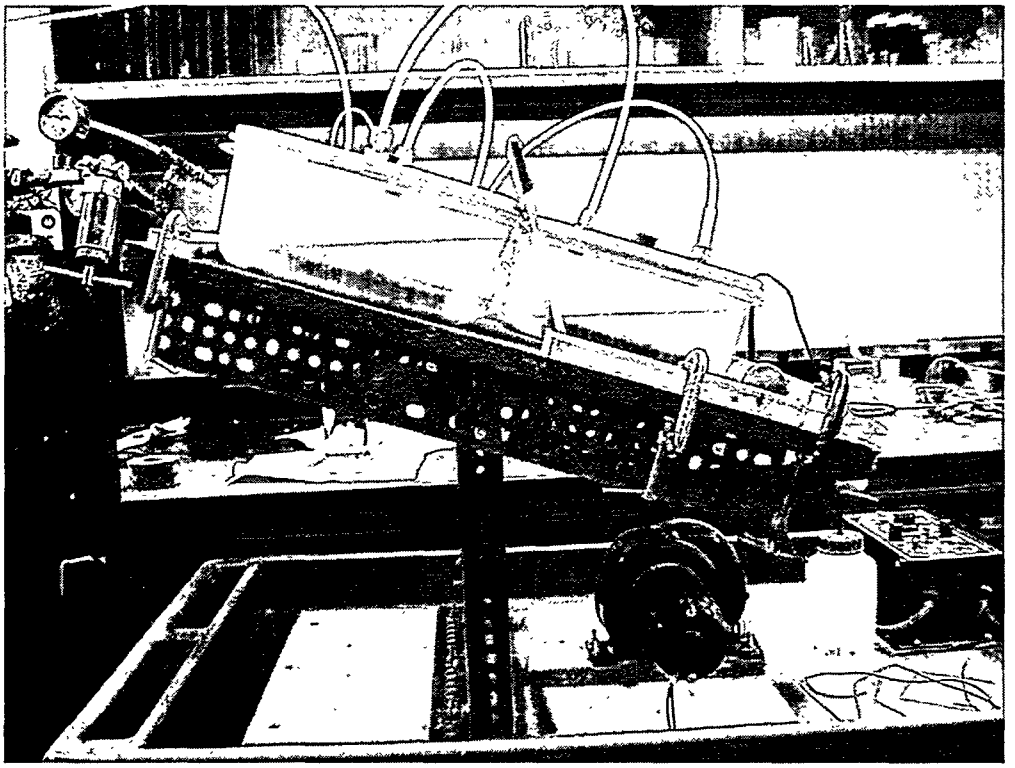

Figure 5: Oscillating Table for controlled calcium leaching

specimens, it turned out that the aggressive solution had not to be renewed during the leaching experiment. Along the leaching process, samples were taken out of the aggressive bath to determine visually the progress of the dissolution front. A square root of time function for the dissolution front progress was obtained being of the order of $\xi_{d1} = 2\ mm/\sqrt{day}$. If we take for reference the "natural" progress of the propagation front of $\xi_{d0} = 0.115\ mm/\sqrt{day}$ (see e.g. [3]), we obtain with a 6M ammonium nitrate solution (480 g/kg of solution), an overall acceleration of $a = 300$ according Eq. (2). For the 11.5 mm in diameter cylinder samples, the dissolution front reached the center of the specimens in less than 9 days. However, additional XRF analysis showed that the average bulk calcium content was still decreasing significantly thereafter. The quasi steady state, i.e. homogeneous calcium content, required 45 days of accelerated leaching.

Triaxial Test Setup

The triaxial cell used in the experiments has a high-pressure steel chamber. The confinement pressure was applied by oil through a latex membrane. The hydrostatic confinement pressure was applied first before the deviator is added until failure. The load rate is constant and the vertical stress measured by an internal load cell.

Triaxial testing started after 45 days of leaching. To avoid the development of

	f_c [MPa]	var [%]	δ_c
Unleached	54.1	5.6	0.82
Leached	5.1	8.3	0.23

Table 1: Compressive strength f_c, coefficient of variation var, and friction coefficient δ_c.

expansive calcium nitro-aluminate products [3,8], the degraded samples were kept in the bath until being tested. To have smooth surfaces and parallel ends, the specimens were cut with a diamond saw to a size of 11.5 × 23.5 mm. Confinement pressures up to 10 MPa were applied. An important issue arises when it comes to triaxial testing of calcium depleted cement pastes, related to chemical damage, i.e. the irreversible loss of elastic stiffness, due to calcium dissolution. This chemical damage leads to a bulk modulus of the degraded material sample, which is of the same order as the compressibility modulus of the interstitial solution, say 2 GPa. Hence, in contrast to undegraded cementious materials, the pore pressure in the interstitial space plays an important role on both deformability, and intrinsic strength of the material. To account for this effect, the triaxial tests were carried out under both drained and undrained conditions. The drained conditions were assured by a dry filter stone at the base of the sample.

Results

Figures 6 and 7 show the results of this test campaign in the $\sqrt{\frac{J_2}{3}} \times \sigma_m$ stress invariant halfplane. In the triaxial test, the second deviator invariant is $\sqrt{J_2} = \sqrt{3} \times |\sigma_v - \sigma_r|$, and the mean stress $\sigma_m = \frac{1}{3}(\sigma_v + 2\sigma_r)$. In figure 7, both invariants are normalized by the uniaxial compression strength. The uniaxial compression strengths for the leached and the unleached paste are summarized in Table 1.

Unleached Cement Paste

Figure 6 shows the well known frictional behavior of cementitious materials under triaxial stress states: Increasing the confinement pressure leads to a significant higher second deviator invariant that the material can support. The friction coefficient that characterizes this property is on the order of $\delta_c = 0.82$.

Leached Cement Paste

The leached samples show a more diverse behavior. We note the important overall strength loss, related to a chemical decohesion. Both, the drained an undrained experiments show a significant strength loss: In uniaxial compression, the chemical decohesion leads to a strength loss of about ninety percent (see Table 1). In addition, a significant difference in the frictional behavior of drained and undrained samples is observed:

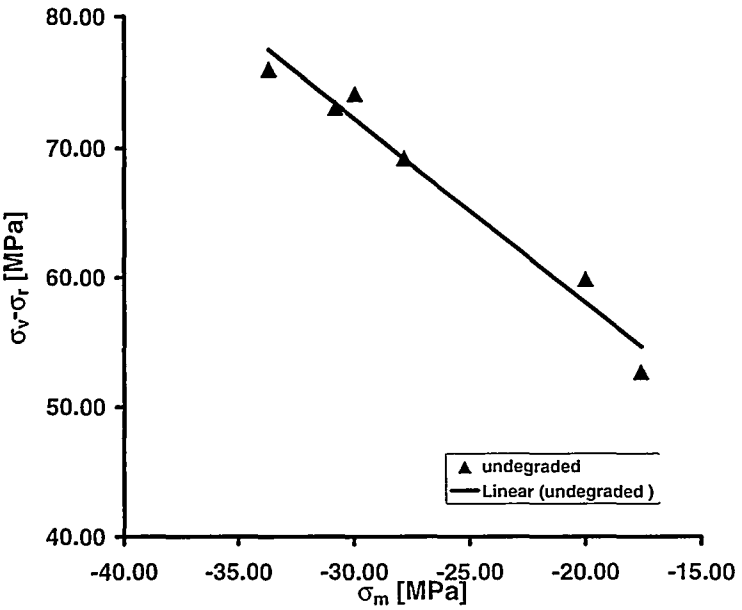

Figure 6: Undegraded paste in deviator-mean stress plane

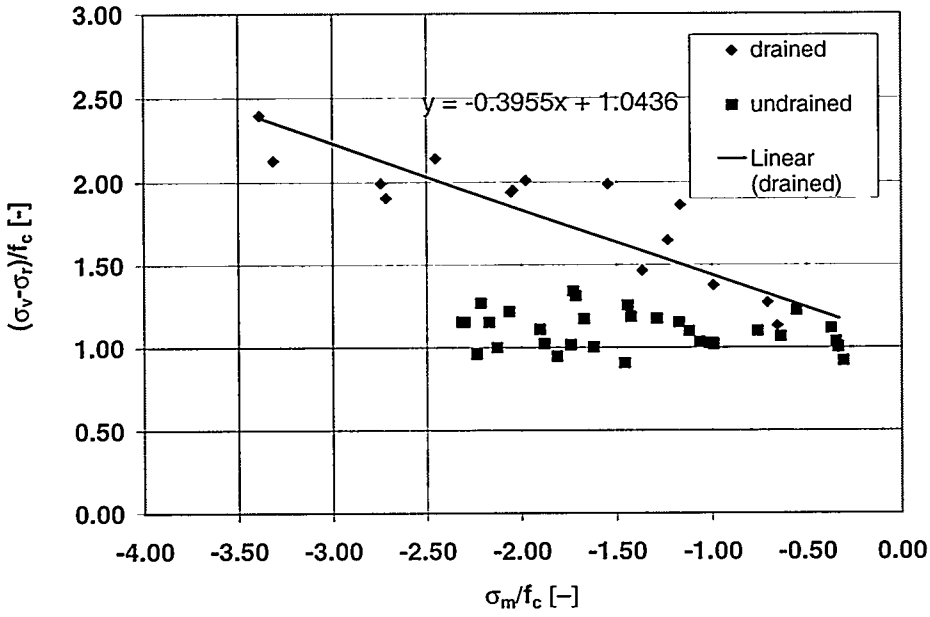

Figure 7: Degraded paste in deviator-mean stress plane (Drained and undrained)

- In the drained case (see figure 7), the linearized friction coefficient is considerably smaller than the one of the undegraded material (in average $\delta_c = 0.23$). This chemically induced loss of frictional behavior can be attributed to the complete dissolution of Portlandite during leaching. The remaining C-S-H particles have a characteristic size 10 to 100 times smaller than the one of Portlandite [4,5]. Consequently, the friction that is mobilized at the grain interfaces during deviator loading (by e.g. interlocking, intergranular stress transfer, etc.) is strongly reduced, leading to a smaller overall pressure dependency of the triaxial material strength response.

- Under undrained conditions, no apparent frictional strength enhancement is observed (figure 7). This can be ascribed to pore pressure effects. The volumetric strain induced by the externally applied confinement pressure, results in pore pressures, which cannot escape in the undrained case. This internal pressure build-up reduces the "effective" confinement stress of the skeleton, which therefore cannot mobilize friction in the material during deviator loading. The constant second deviator invariant for different confinement levels suggests that the pore pressures are of the order of magnitude of the applied confinement pressure, that is up to 10 MPa. This observation underlines the importance of the interstitial pressure in calcium depleted cementitious materials, which originates from the chemical damage undergone by the material during calcium leaching.

Milestone plan

The initial milestone plan remains valid; no changes were necessary.

Task listing

No task has been finished yet. Planned completion dates remain unchanged

Cost performance

Due to accumulation of different expenses, in February 2000 the actual costs exceeded the planned costs by far(see fig.8). We remain nevertheless optimistic that the planned annual budget will be respected.

References

[1] M.Buil, E.Revertegat, J.Oliver, Modeling cement attack by pure water, in: Int. Symp. On Stabilization /Solidification of Hazardous, Radioactive and Mixed Wastes, Williamsburg, 1990.

[2] C.Carde, R.Francois, J.M.Torrenti, Leaching of both calcium hydroxide and C-S-H from cement paste: Modeling the mechanical behavior, Cem Concr Res 26 (8) (1996) 1257-1268.

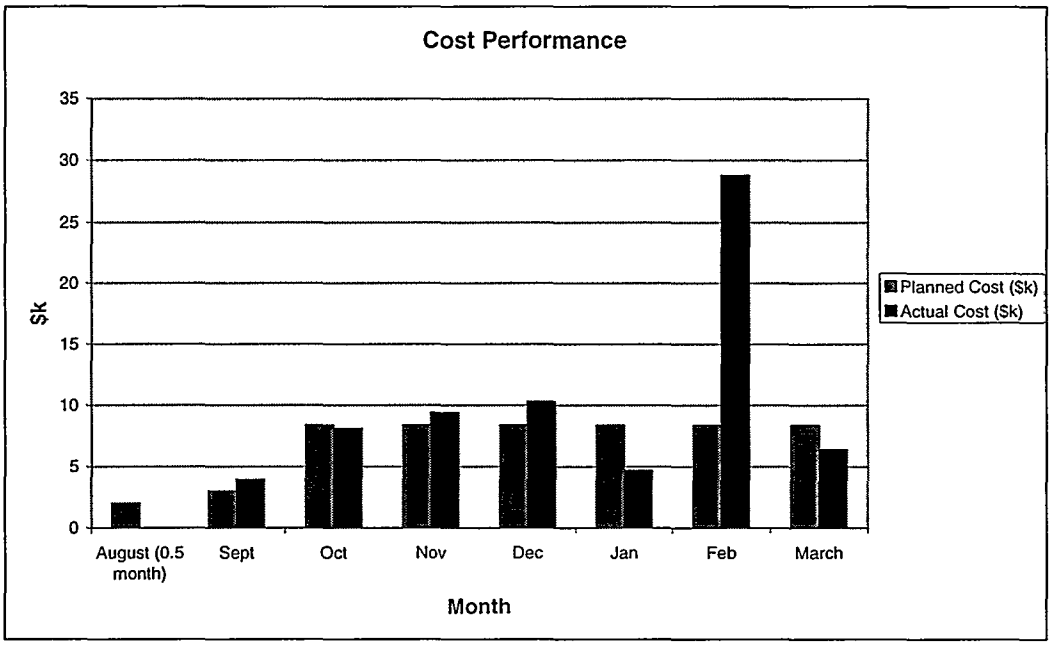

Figure 8: Financial performance

[3] C.Carde, R.Francois, Effect of the leaching of calcium hydroxide from cement paste on mechanical and physical properties, Cem Concr Res 27 (4) (1997) 539-550.
[4] H.F.W Taylor, Cement Chemistry, 2nd edition, Thomas Telford, London, 1997.
[5] I. Jawed, J. Skalny, J.F. Young, Hydration of Portland Cement, in: P.Barnes (Ed.), Structure and Performance of cements, Applied Science Publishers, London, 1983, pp 237-318.
[6] F. -J.Ulm, J. -M. Torrenti, F.Adenot, Chemoporoplasticity of Calcium Leaching in Concrete, J.Engrg. Mech., ASCE, 125(10), 1200-1211.
[7] M.Mainguy, O.Coussy, Propagation fronts during calcium leaching and chloride penetration, J.Engrg. Mech., ASCE, 126 (3), 250-257.
[8] F.M. Lea, The action of ammonium nitrate salts on concrete, M Conc Res, 17 (52), 1965.
[9] B. Gérard, Contribution des couplages mecanique-chimie-transfert dans la tenue a long terme des ouvrages de stockage des dechets radioactifs, Ph.D.-thesis, ENS de Cachan, 1996 (in French).